Fixed-Time Extended State Observer Based Sliding Mode Control Design for Voltage Stability of Island Microgrid

Weiping Wen, Baoqing Niu, Anqi Xu, Xu Guo, and Yanling Shang

***Abstract*—To address the problem of voltage instability caused by uncertain factors including system parameter variations and fluctuating loads, a robust voltage control approach is suggested in this paper with the ideas of sliding mode control (SMC) and fixed-time extended state observer (FxTESO). Initially, a state-space model is constructed by treating both internal and external disturbances as a combined uncertainty term. Subsequently, the conventional linear extended state observer is refined to develop the FxTESO, enabling accurate estimation of system uncertainties. A sliding mode controller is then designed to ensure precise and rapid tracking of the reference voltage while improving the system's disturbance rejection capability. Simulation experiments demonstrate the efficacy of the proposed strategy, confirming its ability to effectively counteract both internal and external disturbances in the microgrid system.**

***Index Terms*—Island microgrid; sliding mode control; extended state observer; fixed-time**

I. INTRODUCTION

With the development and application of photovoltaic, wind energy and other distributed power generation technologies, microgrid systems have received increasing attention in recent years [1, 2]. From the perspective of composition, a microgrid is a self-contained power system with localized control, integrating distributed energy resources (DERs), loads, energy storage systems, and control devices. It can function either connected to the main grid or autonomously in islanded mode [3-5]. For an island microgrid, the system output voltage is often affected by various factors such as changes in system parameters and power loads, which results in the uncertain fluctuations in the output voltage of the system, and reduces the power quality [6]. Therefore, for the precise control of microgrid systems, it has key theoretical and engineering value to study an inverter control strategy of island microgrid with high robustness and minimal steady-state deviation.

Existing studies on disturbance suppression in microgrid inverter systems primarily adopt four key approaches: (1) artificial intelligence-based control strategies, (2) robust control techniques, (3) nonlinear control methodologies, and (4) observer-based disturbance compensation schemes [7-12]. Among these, Reference [7] introduces an advanced control solution using a super-twisting higher-order sliding mode algorithm. By constructing a sliding mode power converter without chattering, the high-order sliding mode control converter has good anti-interference and robustness under large disturbance output loads. Reference [8] unconstrained continuous control vectors to predict load current variations, thereby strengthening the inverter system's resilience against external load disturbances. Reference [9] combines MPC voltage controller with a discrete-time SMC current controller to regulation to achieve faster transient recovery of both voltage and current. Reference [10] proposes a fractional-order sliding mode control strategy for piezoelectric actuators based on an extended state observer. By compensating the static hysteresis nonlinearity of the piezoelectric actuator through the inverse model connected in series with the piezoelectric actuator, which processes the high-order unmodeled dynamics and inverse compensation errors through the fractional-order sliding mode control based on the extended state observer, good response and tracking errors can be achieved. However, the above methods have high information redundancy, which increases the complexity of the control system, and thus the differentials used cannot avoid singularities. Reference [11] proposes an adaptive robust voltage control method by aid of a time-varying gain extended state observer. To enhance voltage tracking performance, the dynamic model of a single-phase inverter system is reformulated into a state-space representation considering only matched disturbances. An adaptive super-twisting sliding mode control law is then applied to ensure fast and precise reference voltage tracking. While existing methods, such as the linear ESO-based active disturbance rejection control [12], improve grid-connected inverter robustness, they suffer from significant initial estimation errors in state variables.

Manuscript received March 19, 2025; revised June 16, 2025. This work was the National Natural Science Foundation of Jiangsu Province under grants BK20201469 and BE2021016-5.

Weiping Wen is a lecturer in the School of Physics and Electronic Engineering, Xinxiang University, Xinxiang 453000, China (e-mail: wenwp@126.com).

Baoqing Niu is an associate professor in the School of Mathematics and Statistics, Anyang Normal University, Anyang 451000, China (e-mail: niubq@126.com).

Anqi Xu is a postgraduate student in the School of Automation, Nanjing Institute of Technology, Nanjing 211167, China (email: y00450240304@jit.edu.cn).

Xu Guo is a postgraduate student in the School of Automation, Nanjing Institute of Technology, Nanjing 211167, China (email: y00450240314@jit.edu.cn).

Yanling Shang is an associate professor in the School of Automation, Nanjing Institute of Technology, Nanjing 211167, China (e-mail:hnnhsyl@126.com).

Microgrid inverters are particularly susceptible to modeling inaccuracies, parameter variations, and external disturbances, all of which degrade control performance. To address these challenges, this paper introduces FxTESO based robust sliding mode voltage control strategy. The proposed approach consolidates disturbances into a lumped uncertainty term, which may be estimated using by FxTESO in a real time. A sliding mode controller is then designed to optimize both response speed and system robustness, ensuring accurate voltage tracking under uncertainties. Comparative simulations validate the effectiveness of the given approach in enhancing anti-interference capability for islanded microgrid inverters.

II. Mathematical Model of Microgrid

Without loss of generality, the studied microgrid can be simplified as single-phase microgrid inverter with a front-stage distributed generation (DG) unit, a power inverter, an LC filter, and a load. And for the microgrid system,

- ✧ U_{DC} is the constant DC-side voltage;
- ✧ u_{inv} is the inverter output voltage;
- ✧ i_{inv} is the inverter output current;
- ✧ R_f , is the resistance of the filter;
- ✧ L_f is the r inductor of the filter;
- ✧ C_f is the capacitor of the filter;
- ✧ i_c is the current of the filter capacitor;
- ✧ i_o and u_o represent the microgrid output voltage and current;
- ✧ u_r is the expected reference voltage u_o ;
- ✧ $u \in [-1,1]$ represents the duty cycle of the inverter switch, and $u_{inv} = uU_{DC}$.

With the aid of Kirchhoff's laws, the mathematical models of the studied system can be obtained as:

$$\begin{cases} L_f \dot{i}_{inv} = u_{inv} - u_o - R_f i_{inv} \\ C_f \dot{u}_o = i_{inv} - i_o \end{cases} \tag{1}$$

which is equivalent to

$$\ddot{u}_o = -\frac{R_f}{L_f}\dot{u}_o - \frac{1}{L_f C_f}u_o + \frac{uU_{DC}}{L_f C_f} - \frac{1}{C_f}\dot{i}_o - \frac{R_f}{L_f C_f}i_o \tag{2}$$

Let

$$\begin{cases} \eta_1 = u_r - u_o \\ \eta_2 = \dot{\eta}_1 = \dot{u}_r - \dot{u}_o \end{cases} \tag{3}$$

where u_r is the reference voltage. Furthermore, considering the uncertainty and external interference of the system, from equations (1)-(3), the error state equation of the microgrid system is obtained as:

$$\begin{cases} \dot{\eta}_1 = \eta_2 \\ \dot{\eta}_2 = (f(\eta) + \Delta f(\eta)) + (b + \Delta b)u + D \\ y = \eta_1 \end{cases} \tag{4}$$

where u , y are the system input and output and

$$\begin{cases} f(\eta) = -\dfrac{1}{L_f C_f}\eta_1 - \dfrac{R_f}{L_f}\eta_2 \\ D = \ddot{u}_r + \dfrac{R_f}{L_f}\dot{u}_r + \dfrac{1}{L_f C_f}u_r + \dfrac{1}{C_f}\dot{i}_o + \dfrac{R_f}{L_f C_f}i_o \\ b = -\dfrac{U_{DC}}{L_f C_f} \end{cases} \tag{5}$$

Take d as the lumped uncertainty of the voltage, then the error state equation can be further stated as:

$$\begin{cases} \dot{\eta}_1 = \eta_2 \\ \dot{\eta}_2 = f(\eta) + bu + \mathrm{d} \\ y = \eta_1 \end{cases} \tag{6}$$

where $d = D + \Delta f(x) + \Delta bu$.

Definition 1 [13] . Consider the system

$$\dot{\eta} = \mathrm{f}(\eta) \text{ with } \mathrm{f}(0)=0 \tag{7}$$

where $\mathrm{f}: R^n \to R^n$ is continuous with respect to η . The origin x=0 is globally finite-time stable if it is globally Lyapunov stable and finite-time convergent. By ``finite-time convergence," it means: If, for any initial condition $\eta(0) \in R^n$, there is a settling time T>0 , such that every is defined for $\mathrm{t} \in [0, \mathrm{T})$ and satisfies and $\eta(\mathrm{t})=0$ for any $\mathrm{t} \geq \mathrm{T}$.

Definition 2 [14,15] . The origin of system (7) is globally practically fixed-time stable if it is globally Lyapunov stable and there are a bounded region U and a bounded settling time T>0 such that every solution converges to U within the time T>0 and remains in it forever.

Lemma 1 [14,15] . For the system (7), if there is a continuously differentiable function $V(t)$ such that

$$\dot{V}(t) \leq -c_1 \mathrm{V}^{\alpha}(t) - c_2 \mathrm{V}^{\beta}(t), \forall t \geq 0 \tag{8}$$

where $c_1 > 0$, $c_2 > 0$, $0 < \alpha < 1$ and $\beta > 1$, then the system is fixed-time stable and the settling time t_r satisfies

$$t_r = \frac{1}{c_1(1-\alpha)} + \frac{1}{c_2(\beta - 1)} \tag{9}$$

Remark 1. From Lemma 1 , it is clear that for system (7) if there is a C^1 function $V(t)$ such that

$$\dot{V}(t) \leq -c_1 \mathrm{V}^{\alpha}(t)\alpha - c_2 \mathrm{V}^{\beta}(t) + \mathrm{m}, \forall t \geq 0 \tag{10}$$

where $c_1 > 0$, $c_2 > 0$, $0 < \alpha < 1$, $\beta > 1$ and $m > 0$, then the system is practically fixed-time stable.

III. Controller Design and Stability Analysis

In this section, a FxTESO is given to estimate the lumped uncertainty in the considered system and then a SMC strategy is employed for the fast voltage control of the system.

A. The Design of FxTESO

Before the design, the lumped uncertainty d of this system is taken as a new state $\eta_3 = d$. Set $q(t) = \dot{\eta}_3$ and $M = \sup_{t \in (0,\infty)} |q(t)| < \infty$. Therefore, equation (4) can be rewritten a third-order system:

$$\begin{cases}\dot{\eta}_1 = \eta_2 \\ \dot{\eta}_2 = f(\eta) + bu + \eta_3 \\ \dot{\eta}_3 = q(t) \\ y = \eta_1\end{cases} \tag{11}$$

According to literature [16,17], the mathematical expression of FxTESO can be given as:

$$\begin{cases}\dot{\hat{\eta}}_1 = \hat{\eta}_2 + \varepsilon^2 g_1\left(\dfrac{\eta_1 - \hat{\eta}_1}{\varepsilon^3}\right) \\ \dot{\hat{\eta}}_2 = \hat{\eta}_3 + \varepsilon g_2\left(\dfrac{\eta_1 - \hat{\eta}_1}{\varepsilon^3}\right) + f(\hat{\eta}) + bu \\ \dot{\hat{\eta}}_3 = g_3\left(\dfrac{\eta_1 - \hat{\eta}_1}{\varepsilon^3}\right)\end{cases} \tag{12}$$

where $\hat{\eta}_i$ represents the estimated value of η_i, ε represents the observer gain, the nonlinear functions g_i are defined as

$$g_i(\theta) = \begin{cases}\theta, & t \le T_1 \\ [\theta]^{\lambda_i} = |\theta|^{\lambda_i} sign(\theta), & t > T_1\end{cases} \tag{13}$$

where $\lambda_1 = 1$, $\lambda_{i+1} = \lambda_i + \vartheta$ with $\vartheta \in (-1/3, 0)$ and T_1 is defined later.

Let $\dot{\tilde{\eta}}_i = \eta_i - \hat{\eta}_i$ be the estimation error of FxTESO. Substituting it into equations (11) and (12), one has

$$\begin{cases}\dot{\tilde{\eta}}_1 = \tilde{\eta}_2 - \varepsilon^2 g_1\left(\dfrac{\tilde{\eta}_1}{\varepsilon^3}\right) \\ \dot{\tilde{\eta}}_2 = \tilde{\eta}_3 - \varepsilon g_2\left(\dfrac{\tilde{\eta}_1}{\varepsilon^3}\right) + \tilde{F} \\ \dot{\tilde{\eta}}_3 = q(t) - g_3\left(\dfrac{\tilde{\eta}_1}{\varepsilon^3}\right)\end{cases} \tag{14}$$

where $\tilde{F} = f(\eta) - f(\hat{\eta})$.

Theorem 1: For the system (11), based on the FxTESO (12), the observation error (14) is globally practically fixed-time stable.

Proof: Assume that $f(*)$ is a continuous Lipschitz function, and a positive constant L exists such that the relationship between them satisfies the following equation:

$$|f(\eta) - f(\hat{\eta})| \le L\|\eta - \hat{\eta}\| \tag{15}$$

Let

$$z_i = \tilde{\eta}_i / \varepsilon^{4-i} \tag{16}$$

where $i = 1,2,3,$ then the estimation error is obtained:

$$\begin{cases}\dot{z}_1 = \dfrac{1}{\varepsilon}(z_2 - g_1(z_1)) \\ \dot{z}_2 = \dfrac{1}{\varepsilon}\left(z_3 - g_2(z_1) + \varepsilon\tilde{F}\right) \\ \dot{z}_3 = \dfrac{1}{\varepsilon}(q(t) - g_3(z_1))\end{cases} \tag{17}$$

When $t \le T_1$, the equation (14) becomes

$$\begin{cases}\dot{z}_1 = \dfrac{1}{\varepsilon}(z_2 - z_1) \\ \dot{z}_2 = \dfrac{1}{\varepsilon}\left(z_3 - z_1 + \varepsilon\tilde{F}\right) \\ \dot{z}_3 = \dfrac{1}{\varepsilon}(q(t) - z_1)\end{cases} \tag{18}$$

That is

$$\dot{z} = \frac{1}{\varepsilon}\left(Az + B\varepsilon\tilde{F} + Cq(t)\right) \tag{19}$$

with

$$z = \begin{bmatrix} z_1 \\ z_2 \\ z_3 \end{bmatrix}, \quad A = \begin{bmatrix} -1 & 1 & 0 \\ -1 & 0 & 1 \\ -1 & 0 & 0 \end{bmatrix}, \quad B = \begin{bmatrix} 0 \\ 1 \\ 0 \end{bmatrix}, \quad C = \begin{bmatrix} 0 \\ 0 \\ 1 \end{bmatrix} \tag{20}$$

Since A is a Hurwitz matrix, a symmetric positive definite matrix P exists which satisfies

$$A^T P + PA = -I \tag{21}$$

where I is the identity matrix.

Define

$$V_1(z) = z^T P z \tag{22}$$

the derivative of which is

$$\begin{aligned}\dot{V}_1(z) &= \dot{z}^T P z + z^T P \dot{z} \\ &= \frac{1}{\varepsilon}\left(-z^T z + 2\varepsilon z^T PB\tilde{F} + 2z^T PCq(t)\right) \\ &\le -\frac{1}{\varepsilon}\|z\|^2 + 2z^T PB\left|\tilde{F}\right| + 2\frac{1}{\varepsilon}z^T PCq(t) \\ &\le -\frac{1}{\varepsilon}\|z\|^2 + 2\varepsilon\lambda_{\max}(P)L\|z\|^2 + 2\frac{1}{\varepsilon}\lambda_{\max}(P)M\|z\|\end{aligned} \tag{23}$$

If $2\lambda_{\max}(P)M < \|z\|$, then one can find a constant c such

$$\dot{V}_1(z) \le -c\|z\|^2 \le -\frac{c}{\lambda_{\max}(P)}V_1(z) \tag{24}$$

which means for a given $V_1(0)$ the system state converges to ball domain $\|z\| \le 2\lambda_{\max}(P)M$ within

$$T_1 \le \frac{\lambda_{\max}(P)}{c}\ln\left(\frac{\lambda_{\max}(P)\|z_0\|}{\lambda_{\min}(P)}\right) \tag{25}$$

where z_0 is the initial value of the system.

When $t > T_1$, the equation (14) becomes

$$\begin{cases}\dot{z}_1 = \dfrac{1}{\varepsilon}\left(z_2 - [z_1]^{\lambda_1}\right) \\ \dot{z}_2 = \dfrac{1}{\varepsilon}\left(z_3 - [z_1]^{\lambda_2} + \varepsilon\tilde{F}\right) \\ \dot{z}_3 = \dfrac{1}{\varepsilon}\left(q(t) - [z_1]^{\lambda_3}\right)\end{cases} \tag{26}$$

In this case, the equation (14) and $\|z\| \le 2\lambda_{\max}(P)M$ imply that there is a constant $\hat{L}$ such that

$$|f(x) - f(\hat{x})| \le \hat{L}\left(|\tilde{z}_1|^{\frac{\lambda_1+\vartheta}{\lambda_2}} + |\tilde{z}_2|^{\frac{\lambda_2+\vartheta}{\lambda_2}}\right) \tag{27}$$

With the homogeneous degree theorem, a Lyapunov function V_2 which has homogeneous degree $\gamma = \max\{\lambda_i\}$ is such that

$$\begin{aligned}V_2(z) &\le \beta_1\|z\|_\Delta^\gamma \\ \dot{V}_2(z) &\le -\beta_2\|z\|_\Delta^{\gamma+\vartheta}\end{aligned} \tag{28}$$

where $\|z\|_\Delta = \left(\sum_{i=1}^{3} |z_i|^{2/\lambda_i}\right)^{1/2}$ and β_1, β_2 are positive constants.

Similarly, we have

$$\dot{V}_2(z) \le -\frac{1}{\varepsilon}\beta_2 \|z\|_\Delta^{\gamma+\vartheta} + \frac{\partial V_2}{\partial z}\tilde{F} + \frac{1}{\varepsilon}\frac{\partial V_2}{\partial z}q \tag{29}$$

Note that when $\|z\| < 2\lambda_{\max}(P)M$, there a neighborhood of the origin U such that

$$\|z\|_\Delta \le \|z\|_\Delta^{\vartheta} \tag{30}$$

Then with appropriate ε it can find that

$$\dot{V}_2(z) \le -\beta_3 \|z\|_\Delta^{\gamma+\vartheta} \le -\beta_4 V_2^{\alpha}(z) \tag{31}$$

where $\alpha = (\gamma+\vartheta)/\gamma < 1$ and β_3, β_4 are positive constants.

The equation (31) renders $V_2(z)$ with the initial condition $V_2(T_1) \le M_2$ convergent to neighborhood of the origin U within finite time.

$$T_2 \le \frac{V_2^{(1-\alpha)}(T_1)}{\beta_4(1-\alpha)} \le \frac{M_2^{(1-\alpha)}}{\beta_4(1-\alpha)} \tag{32}$$

As a result, the error dynamics (14) converge to the neighborhood of the origin U in a fixed time

$$\begin{aligned} T &\le T_1 + T_2 \\ &\le \frac{\lambda_{\max}(P)}{c}\ln\left(\frac{\lambda_{\max}(P)\|z_0\|}{\lambda_{\min}(P)}\right) + \frac{M_2^{(1-\alpha)}}{\beta_4(1-\alpha)} \end{aligned} \tag{33}$$

Thus, the proof of Theorem 1 is completed.

B. Design of Sliding Mode Controller Based on FxTESO

To enhance the reaching speed of the system, a fixed time reaching law is designed in this paper:

$$\dot{s} = -k_1[s]^{w_1} - k_2[s]^{w_2} \tag{34}$$

where $k_i > 0\ (i=1,2);\ 0 < w_1 < 1, w_2 > 1.$

Generally, the traditional SMC suffers from the "chattering" problem, especially when the system is subjected to strong disturbances and uncertainties. To effectively reduce the "chattering" of the system, with the FxTESO, the overall sliding surface is set as:

$$s = \dot{\eta}_1 + \int_0^t \left[l_0[\eta_1]^{\upsilon_1} + l_1[\hat{\eta}_2]^{\upsilon_2} \right] d\tau \tag{35}$$

where l_0, l_1, υ_0 and υ_1 are all positive constants.

Differentiating equation (35), we get:

$$\dot{s} = -\frac{1}{L_f C_f}\eta_1 - \frac{R_f}{L_f}\hat{\eta}_2 + bu + \hat{\eta}_3 + l_0[\eta_1]^{\upsilon_1} + l_1[\hat{\eta}_2]^{\upsilon_2} \tag{36}$$

Considering the estimated values of FxTESO, the mathematical expression of the SMC control law is:

$$\begin{aligned} u = -\frac{1}{b}\Big[& -\frac{1}{L_f C_f}\eta_1 - \frac{R_f}{L_f}\hat{\eta}_2 + \hat{\eta}_3 + l_0[\eta_1]^{\upsilon_1} + l_1[\hat{\eta}_2]^{\upsilon_2} \\ & + k_1[s]^{w_1} + k_2[s]^{w_2} \Big] \end{aligned} \tag{37}$$

Theorem 2: Considering the system in equation (11), the FxTESO expression in equation (14), and the integral SMC in equation (37), the tracking error can converge to zero in a fixed time.

Proof: Choose the Lyapunov function as

$$W = \frac{1}{2}s^2 \tag{38}$$

Substituting the equation (33) into it, we can obtain the derivative of W :

$$\begin{aligned} \dot{W} &= s\left[-k_1[s]^{w_1} - k_2[s]^{w_2}\right] \\ &\le -k_1|s|^{w_1+1} - k_2|s|^{w_2+1} \\ &\le -k_1 W^{\frac{w_1+1}{2}} - k_2 W^{\frac{w_2+1}{2}} \end{aligned} \tag{39}$$

Note that

$$\begin{aligned} & 0 < \frac{1+\mathrm{w}_1}{2} < 1 \\ & \frac{1+\mathrm{w}_2}{2} > 1 \end{aligned} \tag{40}$$

Therefore, according to Lemma 1 and equation (39), s can converge to zero in a fixed time T and satisfies the equation:

$$T < \frac{2}{c_1(1-w_1)} + \frac{2}{c_2(w_2-1)} \tag{41}$$

IV. SIMULATION RESULTS AND ANALYSIS

In this section, a single-phase island microgrid control system on the Matlab/Simulink platform is employed to test the effectiveness of the given method . The system electrical parameters are select as shown in Table 1.

TABLE I
System parameters

Parameter	Value
DC voltage U_{dc}	400 V
Filter inductance L_f	2 mH
Filter capacitor C_f	5 μF
Reference voltage amplitude V_m	311 V
Reference voltage frequency f	314 $\mathrm{rad}\cdot s^{-1}$
Load R_f	10 Ω

Fig.1 gives the output response of the system under the control strategy in this paper, and Fig. 2 and Fig.3 give response of the voltage error and current error

The results show that stable output voltage tracking of microgrid inverter system can be achieved, which confirms that the given voltage SMC strategy can effectively resist the internal and external interferences of the system.

V. CONCLUSIONS

An island microgrid robust voltage SMC scheme has been proposed in this paper based on FxTESO to address the voltage instability problem in island microgrids caused by system parameters and load changes. From the simulation and comparison analysis, the following conclusions are drawn:

1) Under the given control strategy, the microgrid system output voltage can track its reference voltage quickly and exhibits good steady state performance.
2) The output voltage of the FxTESO-based controller is able to effectively reduce the transient peak value of the output current and the transient adjustment time.
3) The FxTESO-based control strategy can estimate the uncertainties of filter parameter perturbations and load changes in real time, thus it has stronger resistance to internal and external interference.

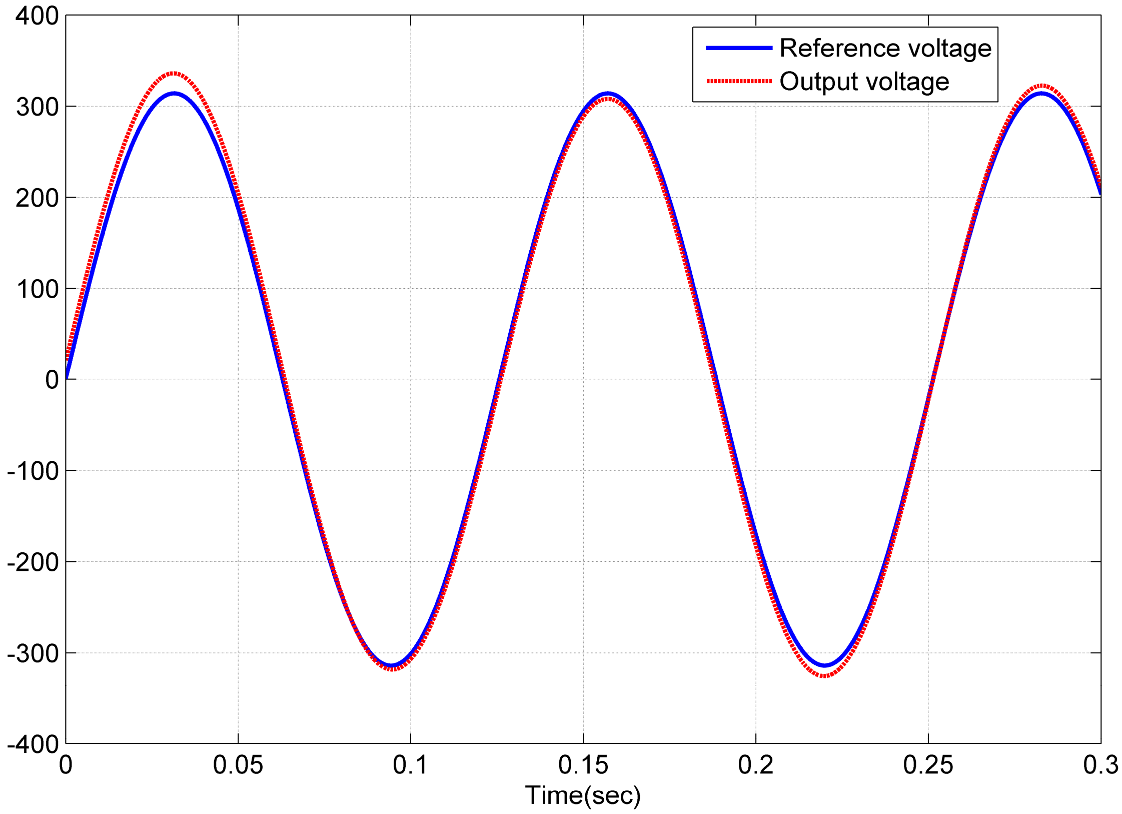

Fig. 1. Response of reference voltage and output voltage.

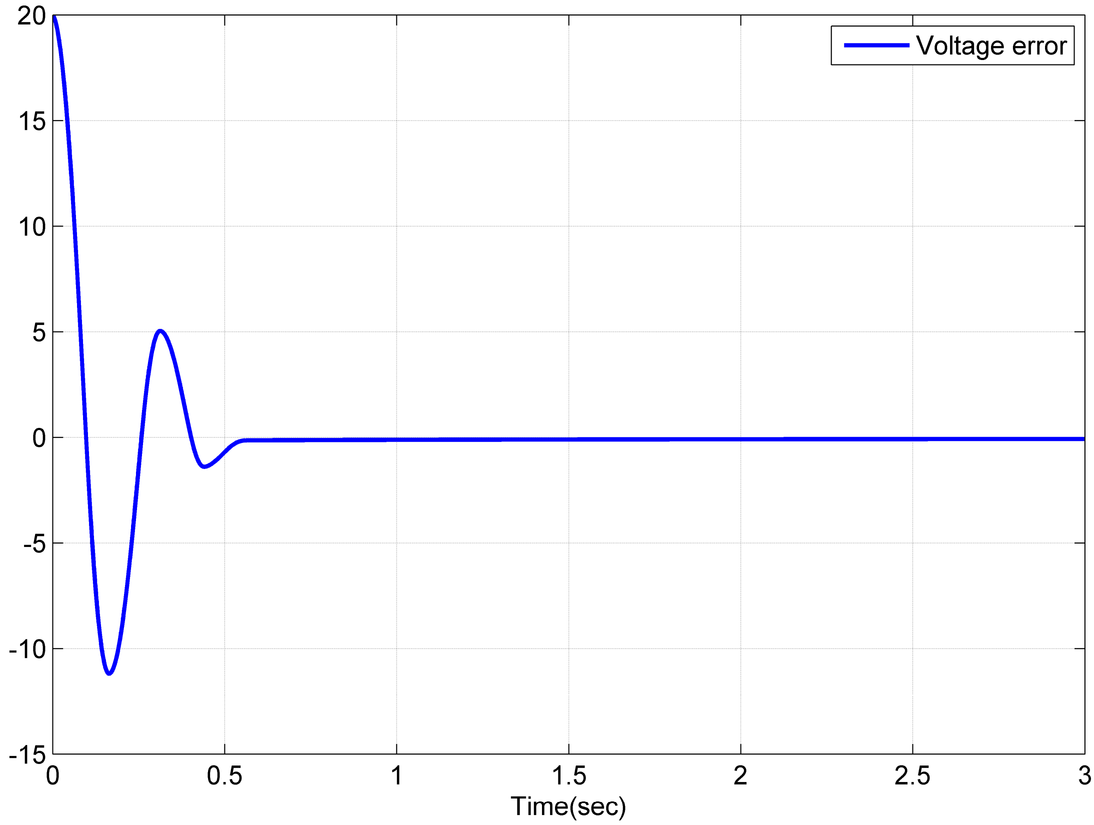

Fig. 2. Voltage error.

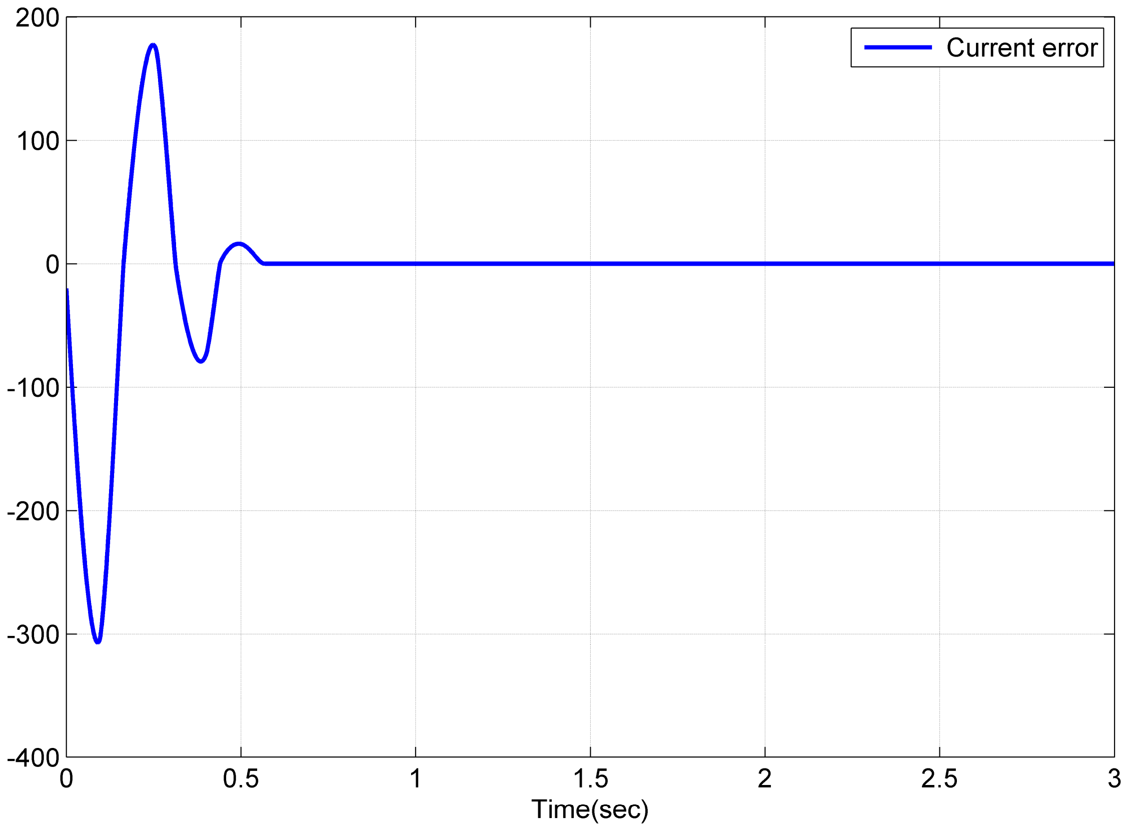

Fig. 3. Current error.

REFERENCES

[1] G. Xie, M. Zhang, M. Yang, D. Wang, "Economic dispatch of isolated microgrids based on enhanced sparrow search algorithm," *Engineering Letters*, vol. 32, no. 4, pp.753-760, 2024.

[2] Y. Wang, Y. Cai, Z. Chang, et al., "An optimal dispatching algorithm of microgrid based on improved particle filter," *IAENG International Journal of Applied Mathematics*, vol. 54, no. 10, pp. 2099-2107, 2024.

[3] S. Leon Felipe, B. Leon Alexis, C. Juan Bernardo, et al., "Modeling and simulation of buck converters and their applications in DC microgrids," *IAENG International Journal of Computer Science*, vol. 48, no. 3, pp. 804-814, 2021.

[4] V. Juan, E. Giraldo, "Hierarchical linear-nonlinear DC microgrid control," *IAENG International Journal of Computer Science*, vol. 48, no. 3, pp. 456-462, 2021.

[5] M. Bueno, G. Eduardo, "Real-time decentralized control of a hardware-in-the-loop microgrid," *IAENG International Journal of Computer Science*, vol. 48, no. 3, pp.653-662, 2021.

[6] N. Vafamand, R. Razavi-Far, M. Arefi, M. Saif, "Fuzzy EKF-based intrusion detection and accurate state estimation of interconnected DC MGs with CPLs," *IEEE Transactions on Power Systems*, vol. 38, no. 6, pp. 5245-5256, 2023.

[7] B. Lu, N. Yi, "Self optimizing distributed reactive power and voltage control strategy for microgrids in islanding mode," *Power System Automation*, vol. 9, pp. 218-225, 2014.

[8] Z. Chen, A. Luo, Y. Chen, et al., "Adaptive sliding mode global robust voltage control method for parallel inverters," *Chinese Journal of Electrical Engineering*, vol. 13, pp. 3272-3282, 2015.

[9] Q. Zhang, C. Peng, Y. Chen, "A control strategy for parallel operation of multiple inverters in microgrids," *Chinese Journal of Electrical Engineering*, vol. 25, pp. 126-132, 2012.

[10] F. Huang, L. Guo, Y. Liang, "High order sliding mode of a robust bidirectional DC conversion device controller," *Control Theory and Applications*, vol. 3, pp. 389-398, 2019.

[11] S. K. Pradhan, D. K. Das, "A robust sliding mode control design for wind-integrated interconnected power system with time-delay and actuator saturation," *Sustainable Energy*, vol. 23, pp. 1566-1572, 2020.

[12] C. Zhang, X. Dou, Z. Zhang, "Photovoltaic high penetration based on the unified structure model of inverters robust adaptive dynamic voltage control for distribution networks," *Chinese Journal of Electrical Engineering*, vol. 22, pp. 7306-7317, 2020.

[13] Y. Shang, J. Huang, X. Shi, X. Zhu, "Global finite-time stabilization for a class of upper-triangular systems subject to input saturation," *Engineering Letters*, vol. 28, no. 1, pp. 16-21, 2020.

[14] A. Polyakov, "Nonlinear feedback design for fixed-time stabilization of linear control systems," *IEEE transactions on Automatic Control*, vol. 57, no. 8, pp. 2106– 2110, 2011.

[15] Y. Cai, Z. Chang, P. Li, et al., "Fixed-time target tracking control of onboard inertially stabilized visual platform system," *IAENG International Journal of Applied Mathematics*, vol. 54, no. 11, pp. 2266-2270, 2024.

[16] H. Pan, Q. Teng, D. Wu, "MESO-based robustness voltage sliding mode control for ac islanded microgrid," *Chinese Journal of Electrical Engineering*, vol. 6, no.2, pp.83-93, 2020.

[17] F. Gao, H. Chen, J. Huang, Y. Wu, "A general fixed-time observer for lower-triangular nonlinear systems," *IEEE Transactions on Circuits and Systems II: Express Briefs*, vol. 68, no. 6, pp. 1992-1996, 2021.